FAST ELECTRON BEAM AND FEL DIAGNOSTICS AT THE ALICE IR-FEL AT DARESBURY LABORATORY

F. Jackson, D. Angal-Kalinin, D. Dunning, J. Jones, A. Kalinin, T. T. Thakker, N. Thompson,
STFC/DL/ASTeC & Cockcroft Institute, Daresbury Laboratory, Warrington, U.K.

Abstract

The ALICE facility at Daresbury Laboratory is an energy recovery based infra-red free electron laser of the oscillator type that has been operational since 2010. Recently fast diagnostics have been installed to perform combined measurements on pulse-by-pulse FEL energy and bunch-by-bunch electron bunch position and arrival time. These measurements have highlighted and quantified fast instabilities in the electron beam and consequently the FEL output, and are presented and discussed here.

INTRODUCTION

ALICE (Accelerators and Lasers In Combined Experiments) at Daresbury Laboratory is a multifunctional accelerator test facility based on an energy recovery linac and includes an infra-red free electron laser (IR-FEL). The IR-FEL achieved first lasing in 2010 [1, 2] and has been studied and used in scientific applications since then.

The ALICE machine includes a DC electron gun photo-injector (producing electrons at 325 keV), a superconducting booster (accelerating electrons to around 6-7 MeV), and an energy recovery loop including a superconducting linac (accelerating the electrons to around 26 MeV), a four-dipole bunch compressor, and arcs composed of triple-bend achromats. The beam is composed of bunch trains 100 μs long, generated at up to 10 Hz repetition rate. The bunch repetition rate within a train is 16.25 MHz (62 ns bunch spacing) and the bunch charge is nominally 60 pC.

The IR-FEL is of the oscillator type and consists of a 40 period undulator around a metre long. The typical FEL wavelength range is 5.5 - 9.0 μm (via adjustable undulator gap), and the FEL delivers an average saturated radiation power of ~ 10 mW, ~4 mJ per macro-pulse, ~3 μJ energy per micro-pulse [2, 3].

Recently the IR-FEL has been utilised for scanning near field optical microscopy [4]. For this application the long term stability (on the $\gtrsim$1 sec timescale) of the FEL is important. The stability of FEL radiation power variations is measured to be 3%, while the wavelength fluctuation is < 20 % of the bandwidth [3].

More recently, new diagnostics have been commissioned at ALICE to measure fast instabilities in FEL and accelerator performance. Fast beam position monitor (BPM) electronics and time of arrival (TOA) monitors have been installed to allow measurement of the positions and TOA of individual bunches within the train. In addition, a photoelectromagnetic (PEM) detector was used to simultaneously record the energy of individual FEL pulses (in this paper the term pulse will be used exclusively to refer to an individual FEL radiation pulse; the term macropulse refers to a ~100 μs train of FEL pulses).

DIAGNOSTIC TECHNIQUES

Several different diagnostics at different locations in the lattice were used simultaneously, as illustrated in Fig. 1. These are described in detail in a previous paper [5] and will be summarised briefly here.

A BPM with bunch-by-bunch capability was located after the first dipole in the return arc (location 'C' in Fig. 1). Bunch positions are computed using standard sum/difference formulae of the processed pickup signals, and the calibration relies on simulations performed previously for the EMMA project [6, 7]. The position resolution is estimated to be 30 μm.

TOA monitors were positioned at locations 'A' (just upstream of the FEL) and 'D' (at re-entry to the linac). These use an optical clock system which has been developed at Daresbury [8] to enable high precision beam TOA monitoring utilising existing BPMs. Timing information of the bunches is converted into amplitude modulation which can be accurately measured on a fast oscilloscope (down to 25 ps resolution, or 40 G samples/sec). Using stripline BPMs the electron bunch arrival times were measured with a single-shot resolution of ~280 fs at location A and ~600 fs at location D.

The energy of individual FEL pulses were measured with a photoelectromagnetic detector (PEM-10.6-1x1 from VIGO Systems S. A.) which has a time constant of < 1 ns. The PEM signal was relayed to another fast oscilloscope and the data post-processed to obtain the integrated signal for each pulse as a measure of the FEL pulse energy.

Synchronisation of the diagnostics was achieved through a combination of analogue triggers and time stamping in EPICS. The measurement is initiated with a beam signal from a pickup before the FEL, which triggers the acquisition of the TOA oscilloscope data at locations A and D (the actual arrival times are obtained with post-processing). This TOA oscilloscope then triggers another fast oscilloscope to acquire the data from the FEL pulse energy monitor. The measurements from both oscilloscopes are time-stamped to the local oscilloscope clock which is synchronised to the main EPICS clock of the accelerator control system. For these measurements the ALICE train repetition rate was set to 1 Hz, which enabled the bunch TOA and FEL pulse energy measurements to be matched to the bunch BPM data which is directly time stamped into EPICS.

ISBN 978-3-95450-126-7

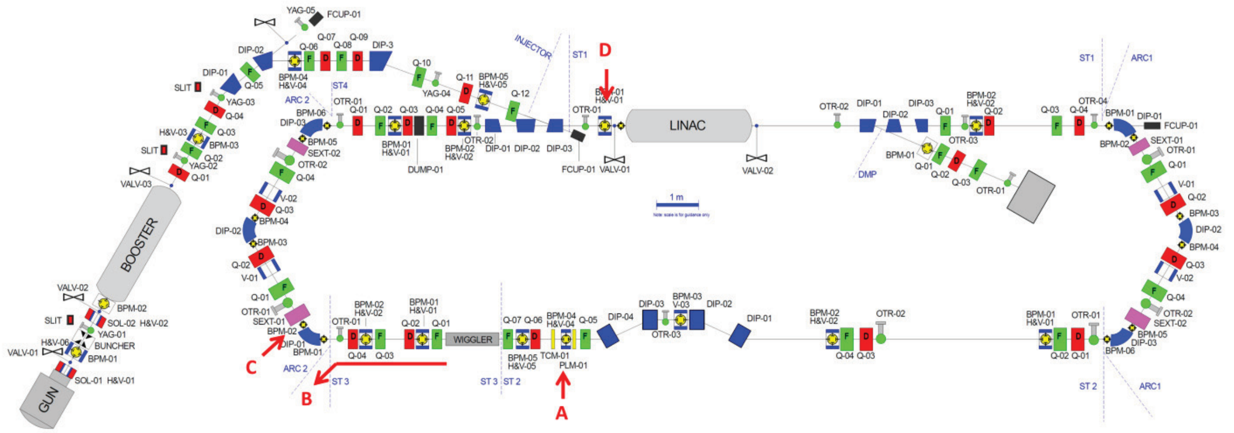

Figure 1. ALICE machine layout with location of fast diagnostics. A) TOA monitor, B) FEL pulse energy monitor, C) BPM @ dispersive location D ~ 30 cm, D) TOA monitor

OBSERVED FEL AND BEAM INSTABILITIES

Around 50 shots (or macropulses) of diagnostic data were recorded, in which the FEL pulse energy, the bunch beam position, and the bunch TOA through the train were measured simultaneously, while varying machine parameters. The machine parameters adjusted included the RF buncher power (in the injector), the arc quadrupoles, and the FEL cavity length.

Gain detuning caused by FEL cavity length adjustment was principally used to delay/advance the saturation time, as shown in Fig. 2 and Fig. 3 and thus observe the instabilities in the lasing and non-lasing regimes.

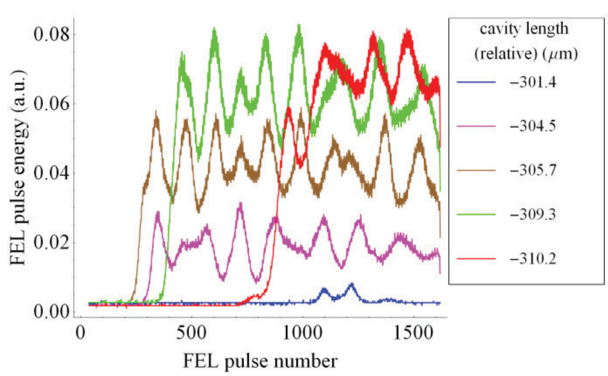

Figure 2: Intra-train FEL pulse energy variation, at different FEL cavity lengths. The equivalent time scale for 1625 pulses is 100 µs.

The rms FEL pulse energy variation during the FEL saturation was measured and is around 10-25%, which seems quite sizable – as can be seen from Fig. 2. However, this does not represent the longer term time-averaged FEL power stability (on a time scale of seconds), which is 3% in optimised conditions [3].

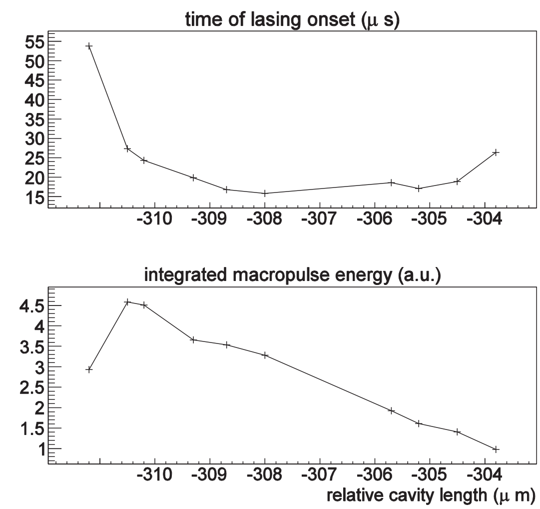

Figure 3: FEL detuning curves obtained using the fast FEL pulse energy diagnostic. The upper plot shows the delay in FEL saturation (a measure of the gain) vs. cavity length; the lower plot shows the train-integrated FEL power vs. cavity length;. By adjusting the cavity length the delay in saturation could be varied allowing beam/FEL instabilities to be measured in the lasing and non-lasing regimes.

Intra-train Instabilities

The pulse/bunch variations in the different (synchronised) observables are shown in Fig 4. for the cases where the FEL is lasing (tuned cavity) and not lasing (detuned cavity).

Clearly, there are several instabilities in all these measurements, and a strong similarity/correlation in the features of the instabilities - (the coincidence of peaks and troughs in the traces can be seen visually). The fourier transforms are shown in Fig. 5 indicating dominant instabilities at specific frequencies, which are ~100-150 kHz and (less pronounced) 300 kHz.

ISBN 978-3-95450-126-7

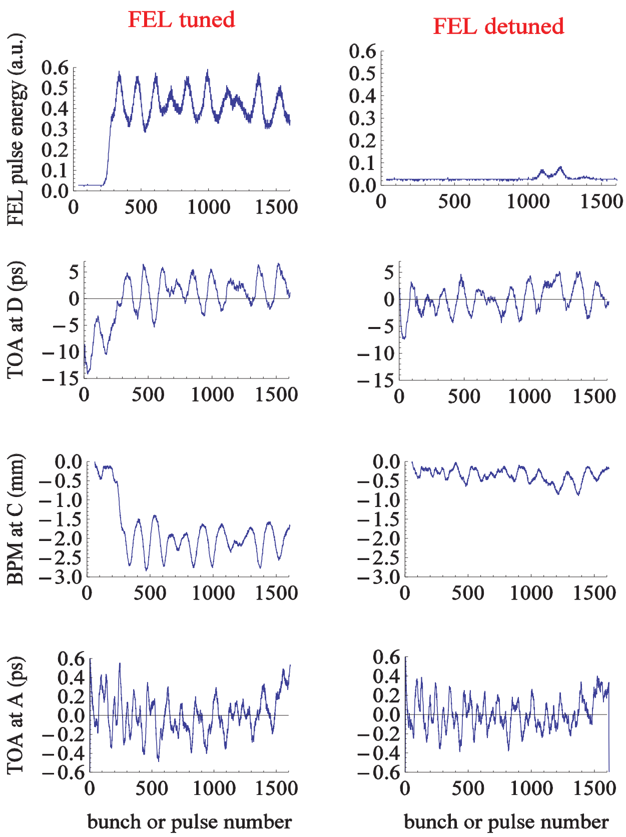

Figure 4: Bunch/pulse diagnostic measurements for the FEL tuned cavity (left) and de-tuned (right). The equivalent time scale for 1625 pulses/bunches is 100 µs.

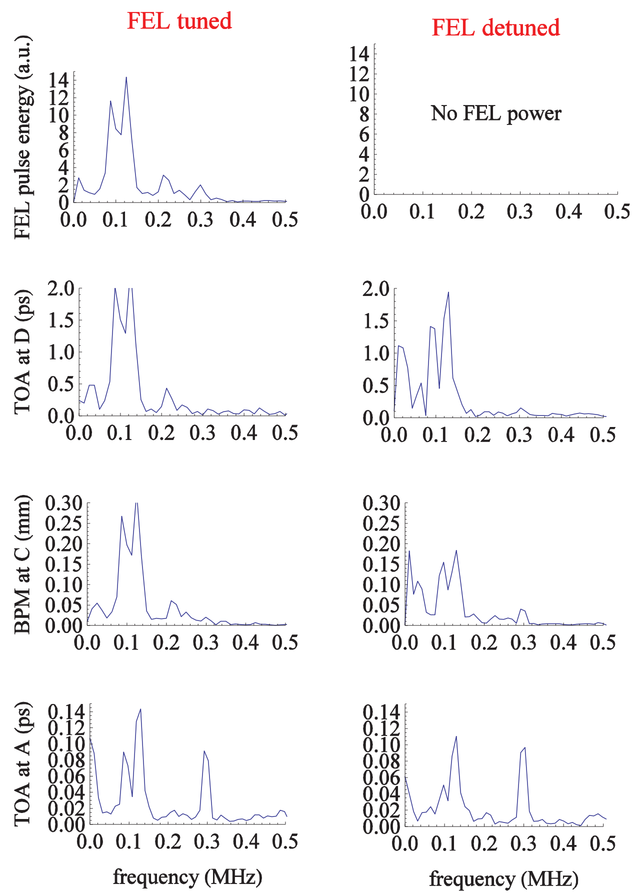

Figure 5: Discrete fourier transform (DFT) of FEL/beam measurements shown in Fig 4. As before, the tuned (lasing) and detuned (non-lasing) measurements are shown on the left and right respectively. (For the tuned measurements, the DFT is taken of only the saturated part of the FEL/bunch train.)

Causes of the FEL Pulse Energy Instability

From previous BPM measurements [9, 10] it is known that bunch position instability exists upstream of the FEL (at the same frequencies as observed here), and is also present in the ALICE injector. The size of the instability depends on the lattice location but can be up to several hundred µm. The exact source of the bunch position instabilities is not yet completely clear. It was suspected that they might originate from jitter of the photoinjector (PI) laser (these kinds of instabilities have been observed elsewhere, for example at the FLASH FEL facility [11]). Other measurements have indicated similarity between PI laser and bunch position instabilities near the electron source [10]. However, the dominant frequencies (100-150 kHz) of bunch position instability seen post-booster and post-linac are much less noticeable compared to the 300 kHz instability upstream of the booster. Thus the exact cause of the bunch position instabilities around ~100-150 kHz remains unconfirmed. However, it is almost certain that the 300 kHz instability is due to instability in the pulse power of the PI laser, since several independent measurements of bunch charge/PI laser pulse charge have all indicated the same instability [10]. In addition previous measurements of the single-side-band phase noise spectra of the PI laser revealed a broadband peak at 300 kHz which is thought to be due to relaxation oscillation in the laser medium [12].

In addition to the previously measured bunch position instability entering the FEL, the measurements presented here also reveal electron bunch TOA instabilities entering the FEL. Although rather difficult to see visually in Fig. 4, some of the features in the TOA instability at location A coincide with those observed in the FEL power.

Both bunch position and timing variations will affect the FEL stability, and this was explored using simulations. Firstly the effect of timing variations was simulated using a modified version of the FELO code [13]. The simulations show that pure sinusoidal timing variations of amplitude 0.1 ps at 100 kHz can cause quite a large oscillation of the FEL output (~20%), as shown in Fig. 6.

The effect of bunch position variations was also simulated using the GENESIS code [14] (in time-independent mode). The results are shown in Fig. 7. They show that a pure sinusoidal bunch position variation of 200 µm can cause a sizeable (~30%) oscillation of the FEL pulse energy. The frequency of the FEL energy oscillations can depend on the offset of the beam with respect to the undulator/optical axis, since this affects the symmetry of the system. In a perfectly aligned system, a

ISBN 978-3-95450-126-7

sinusoidal bunch position oscillation would result in a FEL pulse energy oscillation of twice the frequency of the bunch position oscillation.

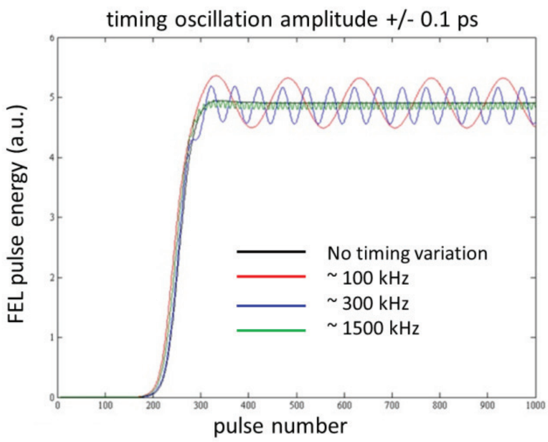

Figure 6: FELO simulation of the effect of bunch timing variations (sinusoidal, amplitude 0.1 ps) on the FEL pulse energy.

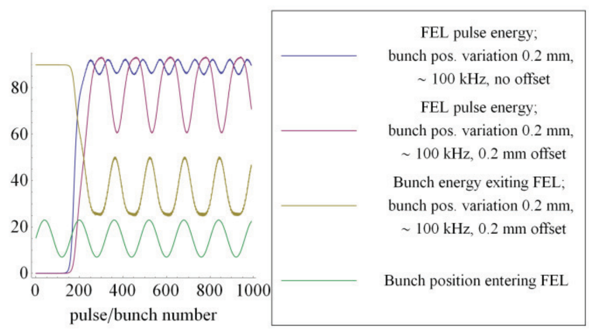

Figure 7: Genesis simulations illustrating the effect of bunch position instability (green) on the FEL output (blue and magenta) and subsequent energy modulation of the bunches (brown). The vertical axis for each plot is arbitrary, although identical for the two FEL pulse energy plots.

Limit Cycle Instabilities

In addition to FEL instabilities caused by bunch position, timing and charge, the FEL may be affected by 'limit cycle' behaviour as observed at the FELIX IR-FEL [15, 16]. In this process sub-pulses evolve in the main FEL radiation pulses due to slippage effects. This leads to the macroscopic effect of modifying the macropulse power envelope, leading to (possibly) similar features to those caused by the electron beam instabilities discussed above. From [15] the frequency of limit cycle oscillations is given by

$$f_{\text{limitcycle}} = \left|\left(\frac{2\delta L}{N\lambda}\right)\left(\frac{c}{2L_C}\right)\right| \qquad (1)$$

where L_C is the FEL cavity length, δL is the cavity detuning, N is the number of undulator periods, λ is the radiation wavelength. In the measurements presented here L_C = 9.22 m, N = 40, λ ~ 10 μm. The absolute values of δL are not known in this experiment since the cavity synchronous length is not known, but theoretically it is expected that $\frac{df_{\text{limitcycle}}}{d(\delta L)}$ ~ 80 kHz/μm, or equivalently if the cavity length is altered by 10 μm (the approximate range in this data), the limit cycle oscillation frequency should change by 800 kHz. The frequency spectra of the FEL macropulse energy are shown in Fig. 8 and there is no frequency feature can be seen to depend on the cavity detuning length in the manner expected of limit cycle oscillations.

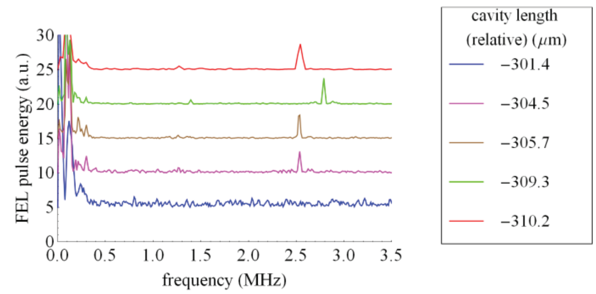

Figure 8: Frequency spectra of FEL macropulse energy at different cavity lengths. The dominant instabilities are at 100-150 kHz and 300 kHz due to beam instabilities. Oscillations due to limit cycle behaviour are not apparent here. The feature at 2.6 MHz may be due to aliasing.

The extent of the limit cycle behaviour is dependent on slippage effects, parameterised by the ratio of the slippage length (number of undulator periods multiplied by the radiation wavelength) to the bunch length. In FELIX this is ratio can be large ($\gtrsim$1) whereas in these experiments on ALICE the ratio is ~ 1. Thus the effect may be smaller in this data and the dominant instabilities seem to be purely due to electron bunch instability.

Enhancement of the Bunch Instability due to the FEL Process.

While the beam instability entering the FEL results in a FEL instability, the FEL in turn affects the beam stability exiting the FEL. For example one can see from Fig. 4 that the bunch position instability in the downstream arc (where the dispersion is ~30 cm) is greater when the FEL is lasing. This can be understood since the FEL pulse energy instability leads to a bunch energy instability (as confirmed in the GENESIS simulations Fig. 7), which is converted into position instability in the dispersive region. This was also confirmed by comparing the DFT of lasing and non-lasing sections of the bunch positions within the same macropulse [10]. From Fig. 4, the FEL does not appear to amplify the TOA variation at location D dramatically. Assuming the amplified TOA instability results again from amplified bunch energy instability, the effect depends on the R_{56} from the FEL exit to the TOA monitor at location D which is small (calculated as ~0.07 m with ELEGANT for the lattice used here) and thus the expected increase in TOA instability at location D is << 1 ps.

ISBN 978-3-95450-126-7

The enhanced beam instabilities downstream of the FEL were not observed to greatly affect the quality of the energy recovery (ER). In general, practical experience with ALICE has shown that ER is relatively easy to maintain during FEL operation. Since ALICE is a low average current machine, and the FEL extraction efficiency is modest, the energy recovery condition is relatively insensitive to these type of instabilities.

Correlation of the Observables

As stated earlier some of the observables of beam and FEL are highly correlated. The correlation of some of the measurements can be understood in terms of lattice transport functions. For example the correlation of the BPM at location C vs the TOA at location D can be estimated since

$$z_D \sim R_{51} x_C + R_{56} \delta_C \tag{2}$$

and if we assume that $x_C = D_C \delta_C$, where $D_C \sim 0.3$ m then

$$z_D = \left(R_{51} + \frac{R_{56}}{D} \right) x_C \tag{3}$$

From ELEGANT simulations R_{51} the R_{56} from BPM to linac entrance are 0.85 and -0.02 m respectively. Thus the correlation $\left(R_{51} + \frac{R_{56}}{D} \right)$ is estimated as approximately 0.80 which is compared to the linear coefficient of the measured correlation of 0.65 as shown in Fig 9.

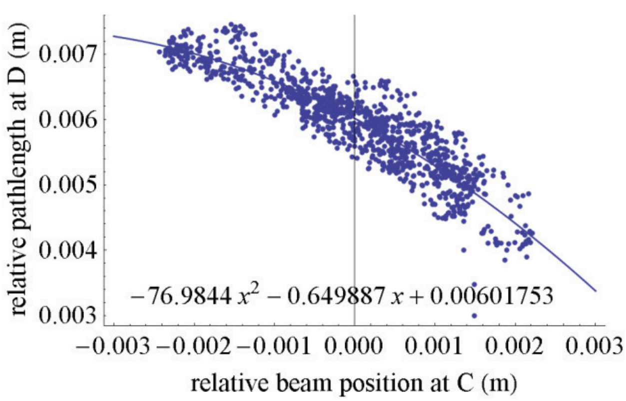

Figure 9: Correlation of relative path length at location D with beam position at location C, during lasing saturation. A parabolic line of best fit is superimposed.

CONCLUSION

The ALICE FEL intra-train pulse energy exhibits instability (sometimes significant) although this does not seriously impact the current FEL applications or the long term FEL stability. The source of this short term instability is a combination of the electron bunch position, charge and timing instability; this is supported by FEL simulations. The timing and position instabilities have a much greater effect than the charge variations, however the relative quantitative contributions of each instability and their correlations have not been evaluated in detail. The origin of the bunch charge instability is the photoinjector laser; however, the source of bunch timing and position instabilities - while suspected to originate from the same source - has not yet been categorically established.

The frequencies of the FEL pulse energy instabilities compared to the bunch position instabilities (observed here and in previously collected data) indicate that the electron beam and the optical axis of the FEL are misaligned in this data.

There is no evidence found in this data for “limit cycle” instabilities in the FEL pulse energy.

REFERENCES

[1] D. Dunning et al, “First Lasing of the ALICE IR-FEL at Daresbury Laboratory”, FEL ’11, Shanghai

[2] N. Thompson et al, “First lasing of the ALICE infra-red Free-Electron Laser”, Nucl. Instr. and Meth. A 680 (2012) 117.

[3] N. Thompson et al, “FEL Research and Development at STFC Daresbury Laboratory”, FEL ’12, Nara.

[4] A.D. Smith et al, “Near-field optical microscopy with an infra-red free electron laser applied to cancer diagnosis”, Appl. Phys. Lett. 102, 053701 (2013).

[5] T. T. Thakker, “Bunch Train Characterisation for an Infra-Red FEL Driven by an Energy Recovery Linac”, IPAC ’13, Shanghai.

[6] S. Machida et al, “Acceleration in the linear non-scaling fixed-field alternating-gradient accelerator EMMA”, Nature Physics 8, 243–247 (2012)

[7] I. W. Kirkman, “Calibration of the EMMA Beam Position Monitors: Position, Charge and Accuracy”, IPAC ’12, New Orleans.

[8] T. T. Ng et al, ‘Optical Clock Distribution System at the ALICE Energy Recovery Linac’, IPAC ’11, San Sebastian.

[9] A. Kalinin et al, “Application of EMMA BPMs to the ALICE Energy Recovery Linac”, IBIC ’12, Tsukuba.

[10] D. Angal-Kalinin et al “ALICE ERL Intra-train Variation Investigation using Bunch-by-Bunch BPMs”, IPAC ’13, Shanghai.

[11] W. Koprek et al, “Intra-train Longitudinal Feedback for Beam Stabilization at FLASH”, FEL ’10, Malmo

[12] G. J. Hirst and L. Jones, “Phase-locking the Photoinjector Laser to the ERLP Accelerator RF”, Report against EUROFEL DS3 Deliverable D3.16.

[13] B. W. J McNeil et al, “FELO: A One-Dimensional Time-Dependent FEL Oscillator Code”, FEL ’06, Berlin.

[14] S. Reiche, “Genesis 1.3: a fully 3D time-dependent FEL simulation code,” Nucl. Instr. and Meth. A 429 (1999) 243

[15] D.A. Jaroszynski et al “Limit cycle behaviour in FELIX” Nuclear Instruments and Methods in Physics Research A 331 (1993) 52-58.

[16] D. A. Jaroszynski, “Experimental observation of limit-cycle oscillations in a short-pulse free-electron laser” Phys. Rev. Lett 70, p3412—3415, 1993.

ISBN 978-3-95450-126-7